Physicochem. Probl. Miner. Process., 61(5), 2025, 210992

http://www.journalssystem.com/ppmp

Physicochemical Problems of Mineral Processing

ISSN 1643-1049

Adsorption behavior of fatty acids during high-density conditioning for spodumene flotation

Brian K. Cook [1,2], Luke Woolcock [1], Baian Almusned [3], and Charlotte E. Gibson [1]

[1] The Robert M. Buchan Department of Mining, Queen's University, Goodwin Hall, 25 Union Street, Kingston, Ontario, Canada K7L 3N6

[2] SGS Canada, 185 Concession St., Lakefield, Ontario, Canada K0L 2H0

[3] Surface Science Western, The University of Western Ontario, 999 Collip Circle, London, Ontario, Canada N6G 0J3

Corresponding author: 9bc25@queensu.ca (Brian K. Cook)

Abstract: The growing demand for electric vehicles and lithium-ion batteries is driving the development of new lithium projects. Spodumene, the primary lithium bearing mineral, is found in pegmatite deposits and is often recovered by froth flotation with fatty acid collectors. These collectors are known for poor selectivity, often recovering other silicate gangue minerals due to their similar surface properties when conditioning is poorly executed. High-density conditioning is a favored approach to achieve desired spodumene flotation performance with tall oil fatty acids, but the mechanisms at play during this stage are largely unknown. This study combined batch flotation with real ore samples and Time of Flight-Secondary Ion Mass Spectroscopy (ToF-SIMS) and X-ray Photoelectron Spectroscopy (XPS) analysis with single minerals, to understand the fatty acid adsorption behavior during conditioning in relation to spodumene flotation performance. The ToF-SIMS results revealed a high amount of physisorbed molecular fatty acid is needed for high spodumene recovery, but physisorption decreased as conditioning progressed, reducing lithium recovery and improving selectivity – an observation validated with two different spodumene ores. This study provides strong evidence that physical adsorption of molecular fatty acid alongside chemisorption of the fatty acid anion, either independently or as an acid-anion complex, are required on spodumene at an ideal ratio for desirable flotation performance.

***Keywords*:** lithium, spodumene, flotation, ToF-SIMS, tall oil fatty acids, physisorption

1. Introduction

Lithium demand is projected to increase in coming years with the uptake of lithium-ion batteries in vehicles and energy storage applications. Lithium comes from 3 sources: brines, hard-rock minerals, and clays. At present, more than half of the world's lithium supply comes from hard-rock deposits containing the lithium-bearing mineral spodumene ($LiAlSi_2O_6$) (Bowell et al., 2020; Jaskula, 2024). Spodumene is an aluminosilicate mineral containing up to 8% Li_2O and is found in hard-rock pegmatites alongside major silicate gangue minerals quartz, feldspars and micas. The main beneficiation processes to concentrate spodumene include ore sorting, dense media separation (DMS), magnetic separation, and froth flotation to produce concentrates grading >6.0% Li_2O and <1.0% Fe_2O_3 suitable for downstream conversion to lithium carbonate and hydroxide for battery applications (Tadesse et al., 2019; McCracken et al., 2021).

The design of a spodumene concentration flowsheet depends on the spodumene grain size across the pegmatite. DMS only flowsheets are suitable for coarse grained deposits, where spodumene liberation is high at particle sizes above 0.5-1.0 mm (Goode et al., 2021; Delboni et al., 2023; McCracken & Cunningham, 2023; Winsome Resources, 2023). When fine-grained spodumene is present – or a wide range of grain sizes exist – froth flotation is used as either the main beneficiation process or in combination with DMS (Redeker, 1981; Bale & May, 1989; Dupéré et al., 2018; McCracken et al., 2021; SRK Consulting, 2023; Boudreau et al., 2024).

DOI: 10.37190/ppmp/210992

The challenges faced by developing spodumene operations often pertain to the flotation circuit. Industrial spodumene flotation flowsheets typically include desliming, magnetic separation, mica flotation, alkaline scrubbing, high-density spodumene conditioning, and spodumene flotation (as shown in Fig. 1), to process feed with a typical particle size between 180 and 250 μm (P_{80}) (Redeker, 1981; Bale & May, 1989; Blanchet et al., 2012; Dupéré et al., 2018; McCracken et al., 2021; Pelletier et al., 2023).

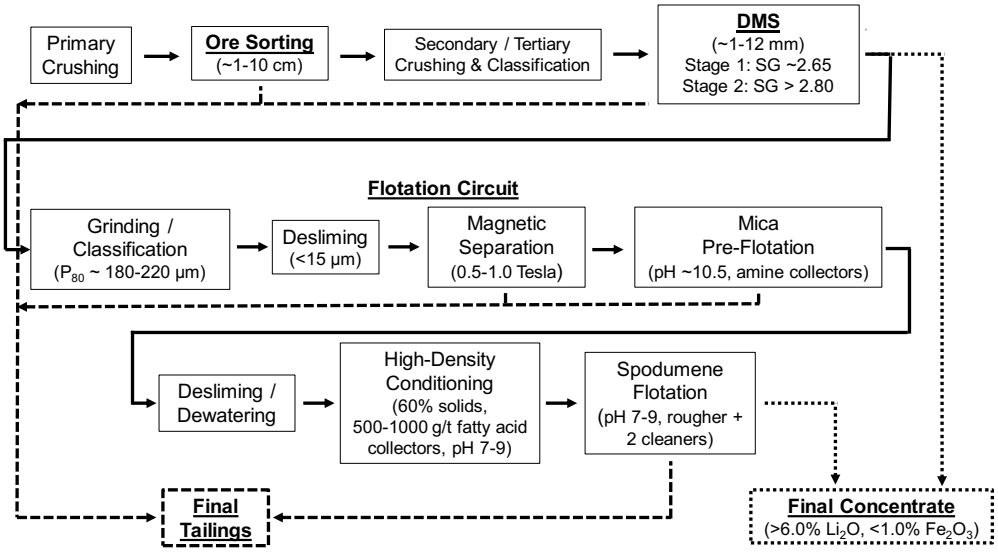

Fig. 1. Block flow diagram of typical hybrid spodumene beneficiation flowsheet using DMS and flotation

The primary collectors used are tall oil fatty acids (TOFAs) – anionic unsaturated carboxylic acids – that usually contain >95% oleic and linoleic acid. Poor selectivity in flotation often occurs due to the poor solubility of fatty acids (Bulatovic, 2007; Kraton Corporation, 2021). It is generally accepted that high-density conditioning with sufficient energy input and residence time will produce desired spodumene flotation performance. But, beyond acknowledging that high pulp densities are needed for adequate dispersion of the insoluble fatty acid, the collector adsorption behaviour throughout conditioning is rarely discussed in literature (Arbiter et al.,1961; Cook et al., 2023, 2024).

Like most silicates, spodumene carries a negative surface charge, which should theoretically make flotation with anionic fatty acid collectors challenging. However, research published by Moon and Fuerstenau (2003) revealed selective spodumene flotation with fatty acids was possible through anionic chemisorption of the fatty acid carboxylate functional group (the primary soluble species in Fig. 2) onto cationic aluminum sites at the mineral surface. The same study also determined the concentration of aluminum adsorption sites was highest on the (110) cleavage plane and that aluminum exposure could be further enhanced by sodium hydroxide (NaOH) scrubbing – which is often included in industrial flowsheets (Fig. 1). More recent research using Density Functional Theory (DFT) reported that a complex of the fatty acid anion (RCOO-) and the molecular acid (RCOOH), referred to as the acid-anion complex (RCOO·RCOOH-), was at maximum concentration around pH 8.5 where spodumene recovery and collector adsorption was highest and is likely the species responsible for flotation (Yu et al., 2015).

Because of this adsorption mechanism, selective rejection of other aluminum-bearing gangue minerals (micas, feldspars, and minor amounts Fe-Al silicates) can be challenging, which is why upstream mica pre-flotation and magnetic separation are often required (Fig. 1). Any remaining micas and Fe-Al silicate minerals (typically hornblendes) remaining in the feed to spodumene flotation can be difficult to reject due to the presence of similar cationic adsorption sites and tendency to float under similar conditions. In addition to upstream rejection of micas and Fe-Al silicates, desliming is also critical for selective spodumene flotation with TOFAs, as they tend to recover fine particles through entrainment and unselective collector adsorption. Because desliming can lead to significant losses in spodumene flotation and other oxide flotation systems, there is growing interest in alternate collectors, or collector blends, that enable selective recovery of fine oxide minerals (Bale & May, 1989; Wen, Miao, Tang, Song, & Feng, 2025).

After upstream processing, the flotation feed should contain mainly quartz, feldspars, and spodumene, with minor amounts of micas and Fe-Al silicates. In this case, feldspars (which also have Al3+ cationic surface sites) are the main competition for fatty acid consumption with spodumene (Gibson et al., 2017; Tanhua et al., 2020; Cook et al., 2023, 2024; Friedman, 2024). Using surface energy calculations, Xu et al. (2016b, 2017) determined preferential adsorption of the anionic fatty acid onto spodumene over feldspars occurs because the order of preferential cleavage planes for spodumene are (110), (001), and (100), while the preferential cleavage planes for albite – a common pegmatite feldspar – are (010), (001) and (110). Adsorption onto spodumene occurs because the highest concentration of aluminum adsorption sites is on the (110) plane of both minerals. However, this advantage is diminished at finer particle sizes as the ratio of concentration of the (110), (100), and (010) cleavage planes approach 1:1:1 (Xu et al., 2016b, 2017).

Other recent studies focus on using cationic activators like Ca^{2+} or Mg^{2+} or using hybrid cationic/anionic collectors to enhance spodumene recovery when using soluble forms of fatty acids like sodium oleate (NaOl) (Jie et al., 2014; Yu et al., 2014; Xu et al., 2016a; Filippov et al., 2019; Tian et al., 2019; Shu et al., 2020; Cao et al., 2021; Jia et al., 2021; Xie et al., 2021a; Zhang et al., 2021; Liu et al., 2023). However, commercial flowsheets, along with reports in the literature, suggest that well executed conditioning (i.e., high pulp density and sufficient energy input, etc.) negates the requirement for cationic activators and hybrid collectors when using TOFAs, and adding these auxiliary reagents may hurt the overall selectivity (Norman & Gieseke, 1940; Munson & Erikson, 1946; Menendez et al., 2004; Cao et al., 2021).

The adsorption behavior of the acid-anion complex has only been studied with NaOl using DFT, which may overlook the challenges associated with TOFA conditioning, including the need for high pulp densities, longer conditioning times, and the sufficient energy input (Arbiter et al., 1961; Cook et al., 2023, 2024). Our recent work highlighted the significance of energy input in the slurry during high-density conditioning and correlated flotation response with the pH behavior. After initial collector addition, the conditioning pH was observed to quickly drop until reaching a minimum around pH 6.6-6.8, then it increased steadily (the rate depending on energy input) until reaching a plateau around pH 7.6. A lower minimum pH of ~6.7 during conditioning (resulting from a lower initial pH or higher collector dosage) and a higher rate of pH increase from the minimum to final pH (resulting from higher energy input) corresponded with improved lithium recovery and concentrate grade, if the final pH was kept around 7.2. At a higher final pH, the concentrate grade was improved but with considerably lower recovery (Cook et al., 2024). The dynamic pH behavior during high-density conditioning and the corresponding changes observed during flotation strongly suggest the collector species in solution and/or adsorbed on the spodumene surface changes over the duration of the high-density conditioning stage.

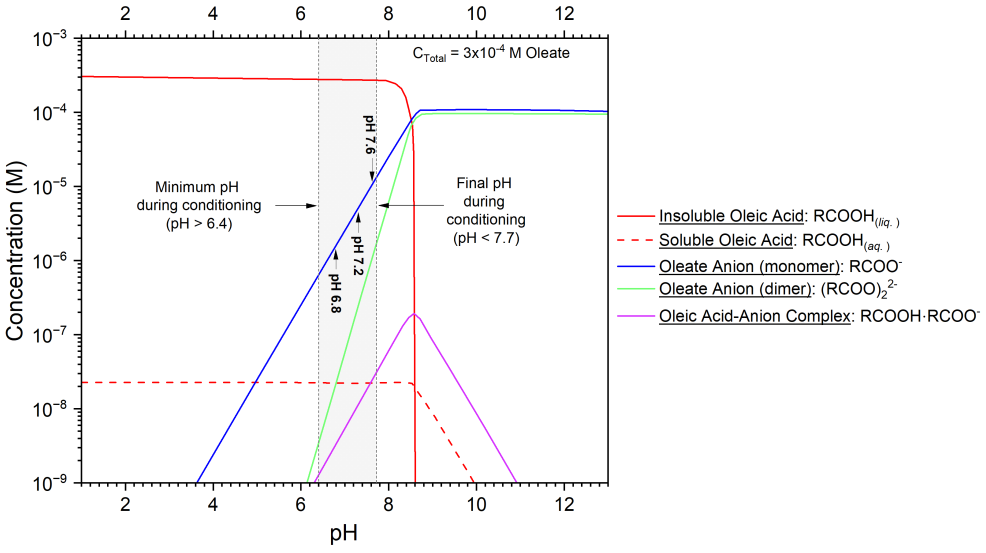

Fig. 2. Oleate species distribution diagram at a total concentration of 0.3 mM NaOl annotated with conditioning pH ranges from previous investigations (Pugh & Stenius, 1985; Zhao et al., 2023; Cook et al., 2024)

To expand this work and evaluate the driving mechanism(s) behind pH changes during fatty acid conditioning, a small-scale high-density conditioning test (60% solids) was designed to mimic larger scale conditioning used in commercial operations. This is the first instance where the adsorption behavior of fatty acids in the spodumene flotation system was investigated using a procedure based on the industrial practice of high-density TOFA conditioning. The objective was to identify changes in collector-particle interactions throughout high-density conditioning on spodumene and other common pegmatite gangue minerals. Collector adsorption behavior was evaluated using X-Ray Photoelectron Spectroscopy (XPS) and Time-of-Flight Secondary Ion Mass Spectroscopy (ToF-SIMS). The findings were supported by batch flotation studies performed on two different spodumene ore samples. The work was conducted to expand the current knowledge base related to fatty acid collector adsorption and to address the challenges during conditioning reported by industrial spodumene operations.

2. Materials and Methods

2.1. Materials

2.1.1. Mineral samples

Seven mineral samples were used in the small-scale conditioning tests and surface characterization studies; three different spodumene samples (Spodumene A, B, and C described below); three common pegmatite gangue minerals (quartz, K-feldspar, and hornblende); and hematite.

Where applicable, lithium assays of the mineral specimens were determined using Inductively Coupled Plasma Optical Emission Spectroscopy (ICP-OES) on an Agilent 5110 ICP-OES, while X-ray Fluorescence (XRF) was performed with a Bruker S8 Tiger WDXRF Series 2 (Billerica, Massachusetts, USA) to determine Al_2O_3, Fe_2O_3, MgO, CaO, K_2O, TiO_2, MnO, Cr_2O_3, V_2O_5, Na_2O, and P_2O_5 assays. Mineralogy was determined using TIMA-X mineralogy performed with a TIMA-X Integrated Mineral Analyzer (TESCAN ORSAY Holding, Brno-Kohoutovice, Czechia) and X-Ray Diffraction with a Bruker AXS D8 Advance Diffractometer (Billerica, Massachusetts, USA). Chemical analysis and mineralogy were all performed at SGS Canada in Lakefield, Ontario. A summary of the different minerals observed and tested in this study, the chemical analysis results, and the mineralogy results are presented in Table 1, Table 2, and Fig. 3, respectively.

Spodumene A (7.12% Li_2O) and B (7.15% Li_2O) were sourced from a heavy medium concentrate produced from a North American deposit. Spodumene A consisted of hand-picked coarse crystals and had the highest spodumene content (95.6%) with quartz as the main impurity (2.4%). Spodumene B was the fraction of the same concentrate too fine for hand sorting, which contained 88.2% spodumene and main impurities of quartz and lepidolite at 6.0 and 3.1%, respectively, with minor amounts of beryl and magnetite; 1.5 and 1.3%, respectively. Spodumene C (87.5% spodumene) was purchased from a private mineral vendor and originally sourced from the Etta Mine in SD, USA. The sample contained 8.1% mizzonite as the main impurity and minor amounts of albite and quartz, at 2.7% and 1.7%, respectively.

Table 1. Chemical formulas of significant minerals found in the two ores and seven mineral samples

Mineral	Formula	Mineral/Ore Sample
Spodumene	$LiAlSi_2O_6$	Spod A-C, Ore A&B
Lepidolite	$K(Li,Al)_3(Al,Si,Rb)_4O_{10}(F,OH)_2$	Spod B, Ore B
Petalite	$LiAl(Si_4O_{10})$	Ore A&B
Cookeite	$LiAl_4(AlSi_3O_{10})(OH)_8$	Ore B
Quartz	SiO_2	Qtz, Hornblende, Spod A-C, Ore A&B
K-Feldspar	$KAlSi_3O_8$	K-Feldspar, Hornblende, Ore A&B
Albite	$NaAlSi_3O_8$	Spod C, Ore A&B
Biotite	$K(Mg,Fe)_3AlSi_3O_{10}(F,OH)_2$	Ore B
Muscovite	$KAl_2(Si_3Al)O_{10}(OH)_2$	Ore A&B
Hematite	Fe_2O_3	Hematite
Hornblende	$Ca_2(Mg,Fe^{2+},Fe^{3+},Al)_5(Al,Fe^{3+})(SiAl)_8O_{22})(OH)_2$	Hornblende, Ore A&B
Mizzonite	$Na_4Al_3Si_9O_{24}Cl$	Spod C

Specimens of quartz, K-feldspar, hornblende, and hematite were all purchased from Boreal Science as mineral samples for research purposes. Only the hornblende sample was submitted for mineralogy due to its anticipated mineral complexity, but later XPS results indicated the hematite contained some minor impurities. The hornblende sample contained 37% actinolite, 27.6% plagioclase, 9.5% diopside, 6.8% quartz and 5.0% k-feldspar.

Table 2. Assays of the spodumene and hornblende mineral samples used for conditioning tests

Assay (%)	Li	Li_2O	SiO_2	Al_2O_3	Fe_2O_3	MgO	CaO	K_2O	TiO_2	MnO	Cr_2O_3	V_2O_5	Na_2O	P_2O_5
Spodumene A	3.31	7.12	63.1	26.3	0.63	0.02	0.03	0.28	0.12	0.01	0.38	0.13	-	-
Spodumene B	3.32	7.15	61.5	26.3	1.00	0.03	0.19	0.19	0.02	0.49	-	-	0.20	1.38
Spodumene C	3.25	6.99	62.9	26.7	0.33	0.03	1.19	0.20	-	0.07	-	-	0.53	0.04
Hornblende	-	-	52.0	11.7	15.9	4.29	8.81	2.63	0.91	1.36	0.16	0.24	0.01	0.07

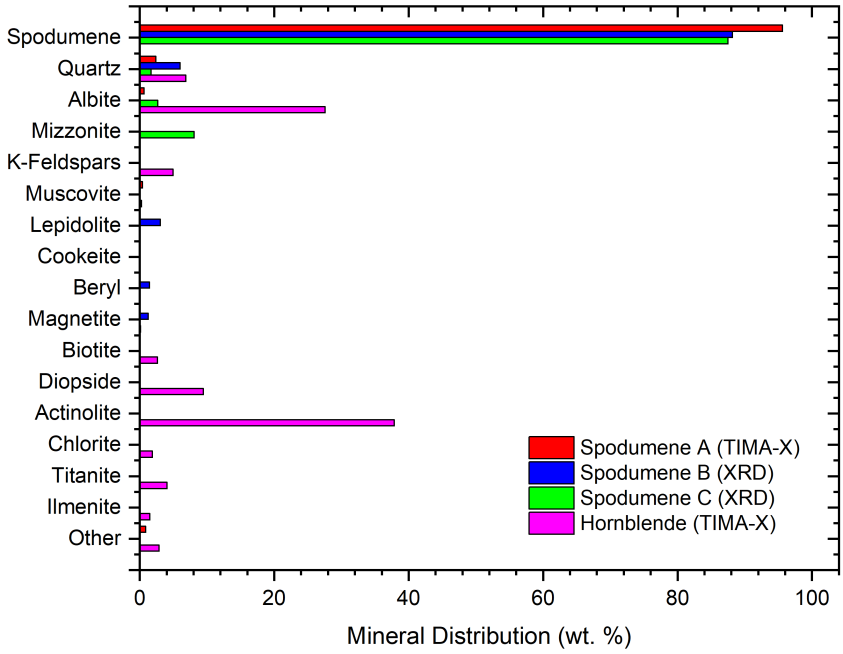

Fig. 3. TIMA-X and XRD mineralogy results of different minerals

2.1.2. Spodumene ore samples

Two spodumene-bearing pegmatite ore samples from different North American deposits were used for batch flotation testing. The head assays and mineralogy of the spodumene flotation feed for both samples are presented in Table 3 and Fig. 4, respectively. Mineralogy analysis of both ores was performed with TIMA-X. Chemical analysis showed the lithium rougher feed of ore A contained 1.64% Li_2O, 0.55% Fe_2O_3, 1.76% K_2O, and 3.87% Na_2O_3, while ore B contained 1.10% Li_2O, 0.75% Fe_2O_3, 1.29% K_2O, and 4.32% Na_2O.

Spodumene was the major lithium mineral in ore A (21.2%) and ore B (15.9%), with minor amounts of other lithium minerals like petalite (0.63% in A and 0.1% in B), lepidolite (0.2% in B), and eucryptite (0.2% in B). Similar gangue mineral content was present in both samples, which included quartz (29.9-34.4%), albite (33.4-37.8%), microcline (6.3-9.8%), muscovite (1.2-1.9%), and hornblende (1.1-1.3%), and minor amounts of chlorapatite (0.9%) and biotite (0.5%) in ore B.

Table 3. ICP and XRF Chemical analysis of the spodumene flotation feed samples

Assay (%)	Li_2O	SiO_2	Al_2O_3	Fe_2O_3	MgO	CaO	K_2O	MnO	Na_2O	P_2O_5
Ore A	1.64	75.2	15.3	0.55	0.20	0.44	1.76	0.05	3.87	0.16
Ore B	1.10	76.7	14.0	0.75	0.20	0.93	1.29	0.05	4.31	0.21

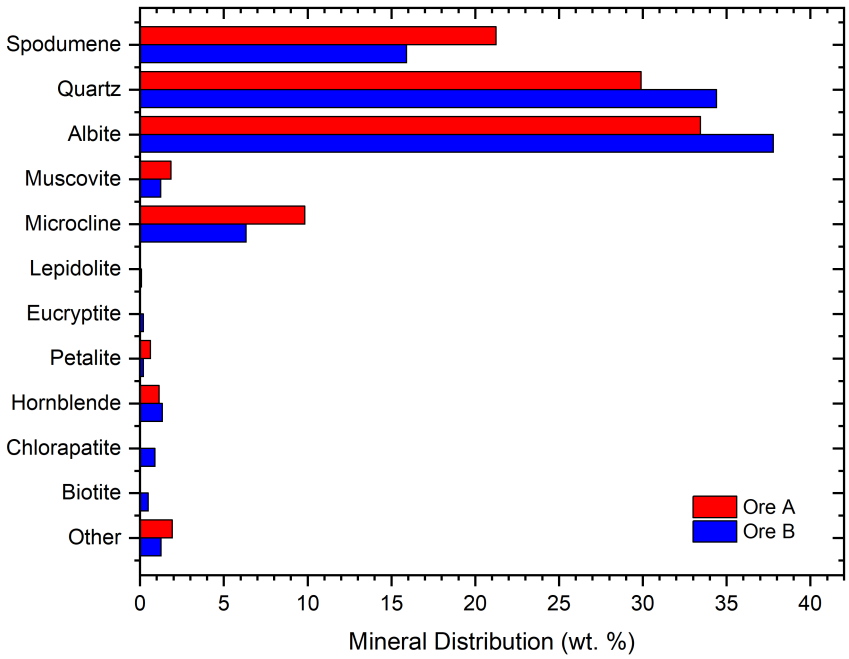

Fig. 4. TIMA-X mineralogy for ore A and B

2.1.3. Reagents

The reagents used included modifiers, activators, and flotation collectors. The pH modifiers included sodium hydroxide (NaOH), sodium carbonate (Na_2CO_3 or soda ash), and hydrochloric acid (HCl), while Pionera F220, an organic biopolymer, was another modifier used as a dispersant. NaOH was supplied by MilliporeSigma™, while soda ash and HCl were supplied by Sigma Aldrich. The only activator used was iron (III) chloride ($FeCl_3$) from Sigma Aldrich. The spodumene flotation collector was Sylfat 'FA2', a TOFA supplied by Kraton. In all experiments, FA2 was added to the pulp during conditioning in its pure form, while the pH modifiers and $FeCl_3$ were used at concentration levels between 0.05 and 5.0%. The exact concentration of the prepared solutions depended on the required dosage or volume of the experiment.

2.2. Experimental methods

2.2.1. Mineral sample preparation

The preparation of mineral samples targeted a particle size range similar to what is used in the flotation of real spodumene ores after desliming (-300/+38 µm). If needed, specimens were broken in a high-carbon steel pulveriser until the entire sample was -3.3 mm. Short intervals (between 3 and 5 seconds depending on particle size) were used for all pulverizing work to minimize the production of particles under 38 µm, as these were removed during screening. After all material was -3.3 mm, it was thoroughly mixed with DI water for 10 minutes at 1000 rpm, then wet screened with DI water to remove -38 µm particles and any potential iron contamination from the pulveriser. The +38 µm material was filtered and dried at 95 °C, then further pulverized in short intervals with a ceramic pulveriser until all material passed a 300 µm screen. The samples were then wet screened a final time at 38 µm with DI water to remove the fines. The oversize fraction was dried and split into representative sub-samples for testing.

2.2.2. Small-scale high-density conditioning

To best mimic the procedure described in Fig. 1 for lab and commercial scale flotation, the procedure of the single mineral conditioning tests included NaOH scrubbing, dewatering, and high-density conditioning. Mixing at small scale at a pulp density of 60% solids was achieved in the setup shown in Fig. 5. Prior to testing, it was determined that a minimum volume of 47 mL was required to adequately mix the slurry at 60% solids (w/w) and make it possible to measure the pH and observe the pH

behaviour during TOFA conditioning. The mass of each mineral sample was then prepared accordingly, ranging from 44.7 g (K-feldspar) to 47.5 g (spodumene) depending on the mineral specific gravity (s.g.).

To replicate the alkaline scrubbing stage, mineral samples were placed in a standard 250 mL beaker and diluted to 40% solids with DI water prepared to pH 11.2 with NaOH. The slurry was mixed in the beaker on a stir plate for 10 minutes, then dewatered over a 25 µm screen. To ensure the solution pH was under 8.0 before FA2 addition, the sample was diluted and dewatered twice by placing the material in a 1000 mL beaker, filling to 1000 mL with DI water, mixing the sample for 1 minute, and dewatering the sample over the 25 µm screen.

After dewatering, the material was transferred to the baffled 150 mL beaker (Fig. 5) and adjusted to 60% solids with DI water and placed on a Caframo overhead stirrer with a stainless-steel impeller. A pH probe, which was calibrated daily, was placed in the beaker and the impeller speed was set to 800 rpm. The pH was adjusted to 8.5 with NaOH before the addition of 500 g/t FA2 and conditioning for at least 20 minutes. The pH was recorded at intervals of 10 seconds for the first four minutes, then 30 seconds for the remaining sixteen minutes of the 20-minute conditioning period. After conditioning, the sample was screened at 25 µm, the effluent was reserved, and the solids were vacuum filtered and air-dried at ambient temperature. Once dry, the samples were bagged and stored in a freezer to preserve for XPS and ToF-SIMS analyses.

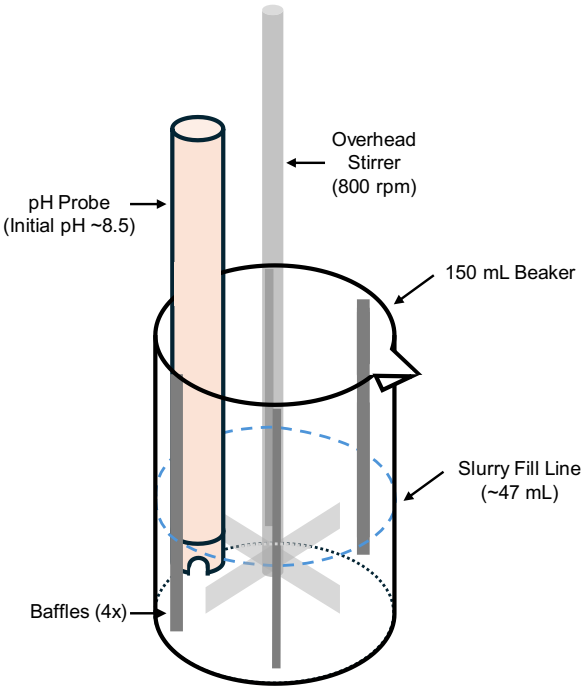

Fig. 5. Schematic of high-density conditioning apparatus with pH probe

2.2.3. X-Ray photoelectron spectroscopy (XPS)

XPS measurements were performed to quantify collector adsorption and evaluate the concentration of cationic metal sites on four samples of spodumene A (conditioned for 0, 2, 7, 20 minutes) and two samples of spodumene C (conditioned for 0 and 20 minutes). Prior to XPS analysis, the treated mineral samples were hand pulverized in an agate mortar and pestle and placed in a vacuum oven at ≤1x10-7 Torr and 50 °C for 5 days to ensure any residual moisture and physically adsorbed oil (or molecular form of the fatty acid) was removed. This was done to measure only the chemisorbed anionic fatty acid species and prevent damage to the XPS chamber from vaporized molecular oleic and linoleic acid, as this occurs at 5.5x10-7 and 8.7x10-7 Torr, respectively (National Center for Biotechnology Information, 2024a, 2024b). Because the The XPS spectra were measured with a Kratos Axis Nova spectrometer equipped with an Al X-Ray source. Each sample was placed onto the mount with double-sided adhesive Cu tape and any excess powder was removed. The mounts were placed onto a coated aluminum platen

and kept under high vacuum 10-8 Torr overnight inside a preparation chamber. Once ready, they were transferred to the analysis chamber of the spectrometer at 10-9 Torr.

XPS data was collected using AlKα radiation at 1486.69 eV (150 W, 10 mA), charge neutralizer and a delay-line detector (DLD) consisting of three multi-channel plates. Binding energies are referred to the adventitious C(sp3) C1s peak at 285 eV. Survey spectra were recorded from -5 to 1200 eV at a pass energy of 160 eV (number of sweeps: 1) using an energy step size of 1 eV and a dwell time of 100 ms. High resolution spectra of O 1s, Ca 2p, C 1s, Si 2p, Al 2p and Li 1s were recorded in the appropriate regions at a pass energy of 20 eV using an energy step size of 0.1 eV. The XPS binding energy error range of the XPS unit used in this study was previously determined to be 0.025 eV based on gold (Au 4f7/2) and copper (Cu 2p3/2) reference peaks.

The spectra were measured using the ESCApe software (Kratos Analytical – A Shimadzu Group Company) and processed using the Computer Aided Surface Analysis for X-ray Photoelectron Spectroscopy (CasaXPS) software (Farley, 2022). The data were corrected for energy shifts due to charging of the sample under the influence of the X-Rays and spectra were corrected for background using the Shirley algorithm (wide scan, high resolution spectra for Na1s) and the Spline Shirley algorithm (high resolution spectra for O 1s, Ca 2p, C 1s, Si 2p, Al 2p, Li 1s). For the quantification, a relative sensitivity factor of 1 was used for each element analyzed. Peak fits were obtained using symmetric line shapes (Gaussian-Lorentzian sum GL(30)) and binding energies are referred to the adventitious carbon C1s peak at 285 eV.

2.2.4 ToF-SIMS

ToF-SIMS was used to qualitatively evaluate the level of collector on the outer layers of the spodumene surface after different periods of high-density conditioning. This was performed at Surface Science Western at the University of Western Ontario, in London, Ontario, Canada. Reference samples of FA2, sodium hydroxide, and the Spodumene A were provided to complete the analysis. To best preserve the molecular species, the samples analysed by ToF-SIMS analysis were air dried and frozen prior to treatment and were not dried in a vacuum oven.

For the ToF-SIMS analyses, a total of 25 grains per sample were examined. Each sample was prepared by rinsing a portion of the sample into a clean glass vial, which was then rinsed repeatedly with DI water, agitated, and decanted to remove fine particles that may interfere with the analysis. The grains were selected using an optical microscope and mounted on an indium foil substrate for analysis.

The instrument used was an ION-TOF, TOF SIMS IV™ secondary ion mass spectrometer. This technique allows for the analysis of the outermost 1-3 atomic layers of a surface by mass spectrometry. A pulsed, 25 keV bismuth primary ion beam BiMn was rastered across an area of interest (roughly 300 μm × 300 μm) on the sample surface at a pixel density of 128 × 128 (2 shots/pixel). The data was collected over 50 scans per area to achieve reasonable signal levels. The bombardment of the surface with primary ion beam induces the emission of positively and negatively charged secondary ions from the sample surface which are then mass analyzed using a time-of-flight mass spectrometer.

The analysis provides a comprehensive survey of the surface species on the mineral grain of interest in the various samples. The analytical approach was to conduct comparative surface analyses of the provided samples to determine statistically significant differences in the surface composition. For the comparative analysis, the intensity (arbitrary units) of selected species detected on the mineral grain surfaces as positive or negative ions were used. All ToF-SIMS data was normalized by the total ion intensity for the region of interest.

2.2.5. Batch flotation

Both ore samples underwent similar bulk processing stages to prepare the spodumene flotation feed, including stage crushing and grinding to a P_{80} of 170 μm for ore A and 210 μm for ore B (grind size selected based on spodumene liberation); desliming to remove fines under 15 μm; wet high-intensity magnetic separation (WHIMS) at 10,000 Gauss; and mica pre-flotation with an amine collector. After mica flotation, the tailings were filtered, homogenized, and dried, before being rotary split into representative 1-kg charges for spodumene batch flotation testing.

A total of ten 1 kg flotation tests are included in this study. Four preliminary repeat scoping tests with ore A were performed to understand the standard deviation, and then the six main tests of this investigation were performed at different conditioning times (three with each ore). Prior to conditioning, each 1 kg charge was scrubbed in a 2 L Denver cell at 1000 rpm, pH 11.2, 50% solids (w/w), and with 250 g/t of Pionera F220 (dispersant) for 10 minutes. The scrubbed feed was then dewatered by diluting and mixing the sample in a 12 L cylinder, allowing it to settle for 7 minutes, and siphoning off the clear water. This was repeated three times for each test to ensure the pulp pH was below 8.0 prior to FA2 addition. The dewatered feed was returned to a 2 L Denver cell and adjusted to 60% solids (w/w), 22 °C and pH 8.3, adjusted with NaOH for high-density conditioning.

For the six main tests of this study high-density fatty acid conditioning was performed at 1300 rpm – or 37 watts per liter (W/L), an initial pH of 8.3, 535 g/t FA2, and three different residence times for each ore type. The residence times were based on the ending conditioning pH (low, baseline, high), where the baseline time was 7 minutes (final pH of 7.1-7.3), the low setting was 3 minutes (final pH of 6.7), and the high setting was 20 minutes (final pH of 7.5-7.7). The four repeat scoping tests with ore A followed the same upstream procedures as the six main tests, but the FA2 conditioning stage was slightly different, being performed at 1000 rpm (27 W/L), an initial pH 8.5, 500 g/t FA2, for 10 minutes. The pH throughout conditioning was continuously recorded at 1-second intervals during all tests. After conditioning, the pulp was diluted to 40% solids and the pH was increased to 8.5 with soda ash for rougher flotation, which was performed for a total of 3 minutes. Each test produced a rougher concentrate and tailings, which were filtered, dried, weighed, and representatively sub-sampled for chemical analysis by ICP and XRF.

3. Results and Discussion

Discussion of the experimental results begins with the dynamic pH behavior during conditioning and how this may relate to collector adsorption on different pegmatite minerals. Next the XPS and ToF-SIMS results of select conditioned samples are presented to evaluate collector adsorption behavior at the mineral surface, with a focus on adsorption changes throughout conditioning. The findings from XPS and ToF-SIMS are then used to explain the changes in batch flotation performance of real spodumene ores, supporting a proposed explanation for the changing pH and collector adsorption at spodumene surfaces during high-density conditioning.

3.1. High-density conditioning pH behavior of single minerals

Much of the existing literature does not explicitly delineate between the pH of conditioning versus the pH during flotation and often omits information regarding pH control (or lack thereof) throughout high-density conditioning. However, during batch flotation testing in previous investigations, a dynamic pH behaviour was observed when the pH was left uncontrolled (Cook et al., 2024). A relationship between the conditioning pH behavior and flotation performance has also been identified. These relationships suggest that changes in pH may stem from changes in collector adsorption during conditioning. Fatty acid species distribution diagrams show that increasing pH in the region where high-density conditioning occurs should increase the concentration of the fatty acid anion and the acid-anion complex, both of which are responsible for spodumene flotation (Pugh & Stenius, 1985; Zhao et al., 2023.

The pH profiles of each sample during conditioning were logged for at least 20 minutes and are presented in Fig. 6 along with the pH characteristics minimum pH, final pH and rate of pH change (Δ pH/min).

The pH profiles shown in Fig. 6 highlight that during conditioning, a common trend was observed for all minerals. This trend had 3 main characteristics: (1) the initial drop in pH after TOFA addition; (2) the minimum pH; and (3) the increase in pH after the minimum until a final plateau. During conditioning, the pH transitioned from a region where, according to Fig. 2, there was very little fatty acid-anion complex or anionic fatty acid and a dominating concentration of molecular fatty acid (pH ~6.5-7.0), into a region where the molecular form still dominated but there was a considerable increase in the concentration of the acid-anion complex and the fatty acid anion (pH ~7.1-7.8). The behavior suggests a change in collector adsorption and speciation throughout conditioning, from the molecular

acid (oil phase) to the anion and the acid-anion complex, which ultimately promotes selective spodumene flotation. Contrary to literature, the pH during conditioning never overlapped with the region in Fig. 2 where the acid-anion complex was at a maximum (pH ~ 8.5), implying that direct adsorption of the acid-anion complex onto spodumene is not the only driver of flotation performance. Instead, the conditioning pH suggests the acid-anion complex formed on the surface during high-density conditioning the ratio of molecular to anionic fatty acid increases. Alternatively, if there is little or no formation (and presence) of the complex in this pH region, as indicated in Fig. 2, spodumene flotation may rely on co-adsorption of both species at the particle surface.

As discussed, the literature indicates that fatty acid collector readily adsorbs at cationic surface sites (Al^{3+}, Fe^{3+}, Ca^{2+}, and Mg^{2+}) on spodumene and other silicate minerals, which drives flotation performance (Moon & Fuerstenau, 2003; Xu et al. 2016b, 2017). In the present study, the rate of pH change increased in the presence of a higher concentration of cationic surface sites. For example, quartz – which theoretically contains no cationic surface sites – had a nearly negligible change in pH during conditioning (Fig. 6). Other minerals common in pegmatites exhibited a higher pH rate of change when more cationic surface sites were present, increasing from K-feldspar to spodumene, and highest for the hornblende sample. The increase from feldspar to spodumene aligns with the observations of Xu et al. (2016b, 2017);the primary spodumene cleavage plane (110) contains a higher concentration of Al sites than the primary feldspar cleavage plane (010), and hornblende can contain several cationic metals in its matrix (Table 1).

Further supporting this relationship, the pH rate of change for quartz increased to a similar rate as K-feldspar after pre-conditioning with 365 g/t of $FeCl_3$, approximately the same dosage used by Jie et al. (2014) (1.5×10^{-4} M) when investigating Fe^{3+} as an activator to increase spodumene recovery. The rate of pH change exhibited by the different minerals of spodumene-bearing pegmatites also aligned with reported flotation behaviour of these minerals: Quartz and feldspars can be selectively rejected but it remains challenging to reject amphiboles like hornblendes (Yu et al., 2014; Liu et al., 2015b; Filippov et al., 2019; Gao et al., 2021; Zhang et al., 2021).

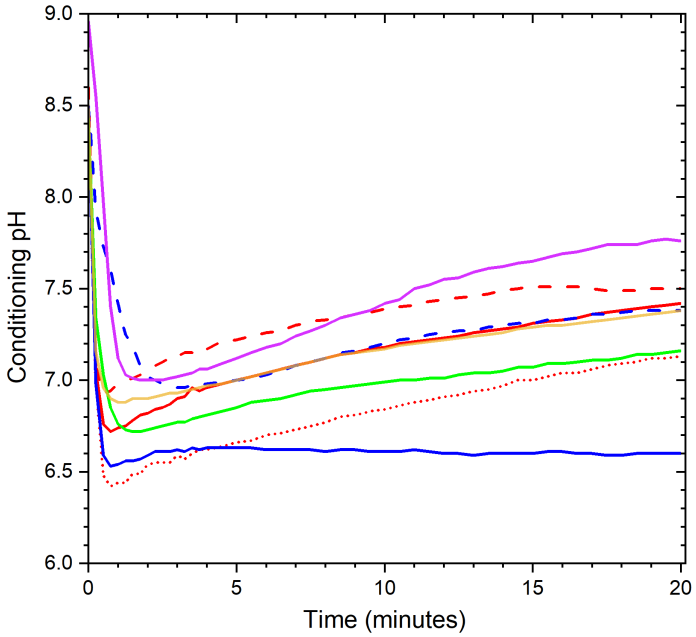

Mineral Sample	Key	Min. pH	Final pH	Rate (Δ pH/min)
Spodumene A		6.72	7.59	0.036
Spodumene B		7.00	7.50	0.037
Spodumene C		6.42	7.13	0.036
Quartz		6.53	6.60	0.005
Quartz + Fe(III)		6.96	7.38	0.028
K-Feldspar		6.72	7.16	0.021
Hornblende		7.00	7.76	0.049
Hematite (No Scrub)		6.90	7.38	0.027

Fig. 6. Conditioning pH profiles of single minerals during high density conditioning tests and corresponding pH characteristics

3.2. Fatty acid adsorption onto different pegmatite minerals

Pure mineral samples from the high-density conditioning tests were analyzed to help explain the dynamic pH behavior and identify differences in fatty acid adsorption at different mineral surfaces. Samples of spodumene A, conditioned for three different times to target final pH values of 6.8, 7.2 and 7.6, were analyzed with XPS and ToF-SIMS to observe any changes in collector adsorption. A sample of

spodumene C and other mineral samples were submitted for XPS analysis after TOFA conditioning for a period of 20 minutes (comparable conditions to Spodumene A conditioned to a final pH of 7.6). The XPS analyses were expected to identify the presence of the fatty acid anion at the different mineral surfaces due to vaporization of the molecular acid after vacuum drying, while ToF-SIMS was expected to identify adsorption differences in the presence of molecular fatty acid (residual oil). The findings of each analytical technique were compared and combined to better understand the collector adsorption behavior during high-density conditioning.

3.2.1. XPS

The XPS results for changes in the atomic concentration of exposed cationic adsorption sites on different mineral samples before and after high-density TOFA conditioning are summarized in Table 4, Fig. 7, and Fig. 8. Shifts were evaluated by taking the difference in binding energy of the treated samples and the corresponding untreated blank samples. Owing to the described vacuum drying treatment prior to XPS that volatized any residual molecular fatty acid, any observed changes can be attributed to chemisorption of the fatty acid anion (monomer and/or dimer) and acid-anion complex.

Table 4 and Fig. 8 show that on the spodumene A and C surfaces after 20 minutes of conditioning in FA2, aluminum decreased by 1.04 and 1.14%, respectively, while lithium decreased by 1.25 and 1.43%, respectively, which are comparable to changes reported in other XPS spodumene studies using NaOl. However, the changes in the lithium and aluminum binding energies for these two samples were subtle, at less than +0.07 eV, suggesting significant chemical interaction with FA2 did not occur, which was not expected based on existing spodumene flotation literature (Yu et al. 2015b; Shu et al., 2020; Meng et al., 2022; Ma et al., 2024; Zhu et al., 2025).

The location of the C 1s orbital corresponding to the C=O and the carboxylate anion provided evidence of FA2 on the surface as these species were only detected on samples conditioned with FA2. In addition, significant energy shifts of +0.58 and +1.06 eV at the C 1s orbital were observed for spodumene A and C after 20 minutes conditioning with FA2, respectively. The observed changes in the carbon bonding environment throughout conditioning (Fig. 8) were attributed to interactions between different fatty acid species, which potentially indicated the presence or formation of the acid-anion complex due to van der Waals forces between molecular and anionic FA2 species (Fukuda et al., 2001; Yu et al., 2015). Although the reported changes in Al binding energy were negligible in this study, anionic chemisorption has been shown in the literature with other studies using NaOl (Yu et al. 2015b; Shu et al., 2020; Meng et al., 2022; Ma et al., 2024; Zhu et al., 2025). It is possible that the use of insoluble TOFA at the tested dosages did not provide a high enough concentration of soluble anionic species to result in the level of chemisorption observed on spodumene when NaOl is used, however further studies are needed to confirm this.

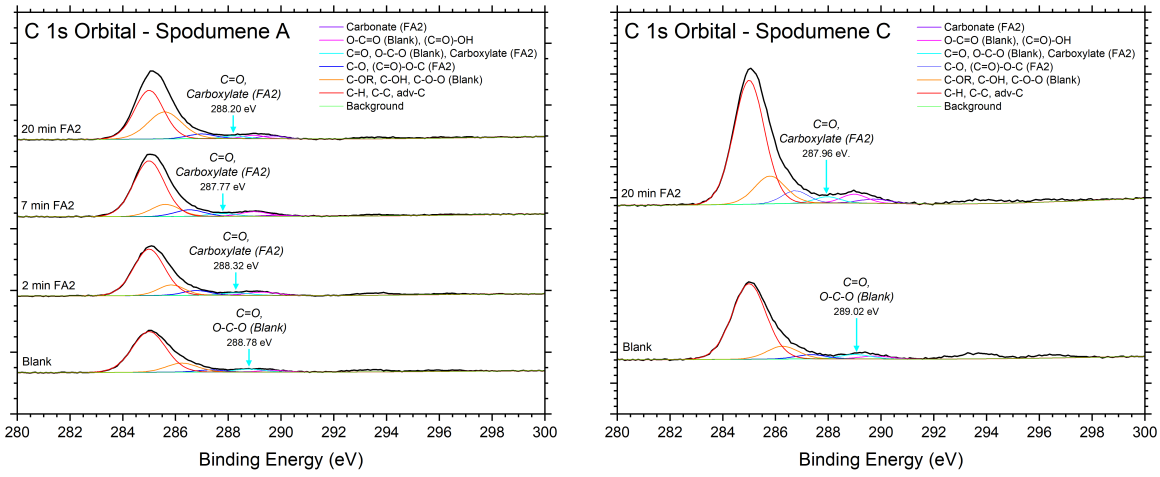

Fig. 7. High resolution XPS spectra for Spodumene A (right) and C (left) at the C 1s orbital before and throughout conditioning with FA2

Shifts in binding energy of spodumene A at the C 1s orbital corresponding to C=O and the carboxylate anion (attributed to FA2) at these time intervals suggest there are continuous changes throughout conditioning. The C 1s binding energies in Fig. 7, attributed to molecular acid-anion interactions, decreased from 288.78 eV without FA2, to 288.32 eV after 2 minutes conditioning and further to 287.77 eV after 7 minutes, then increased back up to 288.2 eV after 20 minutes. The decrease in binding energy after 2 minutes at the C 1s orbital can be attributed to chemisorption of the fatty acid anion onto spodumene, while the increase after 20 minutes conditioning may represent disassociation van der Waals forces between the molecular acid and anion or potential fatty acids chemically bound to the surface (Fukuda et al., 2001; Yu et al., 2015). Both spodumene samples exhibited an overall decrease in binding energy at the C 1s orbital after 20 minutes conditioning, however, because spodumene C was only tested at one time interval the same trend in binding energy changes was not captured.

Table 4. Summary of XPS results for atomic concentration and binding energy

Atomic Concentration (%)

Mineral	Treatment	Al 2p	Li 1s	Mg 2p	Fe 2p3/2[i]	Fe 2p3/2[ii]	C 1s	O 1s
Spodumene A	Blank	9.00	5.52	-	-	-	0.95	15.56
	2 min FA2	8.08	5.85	-	-	-	0.89	13.57
	7 min FA2	8.29	5.46	-	-	-	0.79	16.48
	20 min FA2	7.96	4.27	-	-	-	0.64	16.09
Spodumene C	Blank	9.18	5.63	-	-	-	0.66	18.00
	20 min FA2	8.04	4.20	-	-	-	0.77	15.50

Binding Energy (eV)

Mineral	Treatment	Al 2p	Li 1s	Mg 2p	Fe 2p3/2[i]	Fe 2p3/2[ii]	C 1s	O 1s
Spodumene A	Blank	74.78	56.18	-	-	-	288.78	531.22
	2 min FA2	74.78	56.14	-	-	-	288.32	531.20
	7 min FA2	74.79	56.12	-	-	-	287.77	531.26
	20 min FA2	74.85	56.22	-	-	-	288.20	531.37
Spodumene C	Blank	74.73	56.17	-	-	-	289.02	531.24
	20 min FA2	74.76	56.23	-	-	-	287.96	531.31

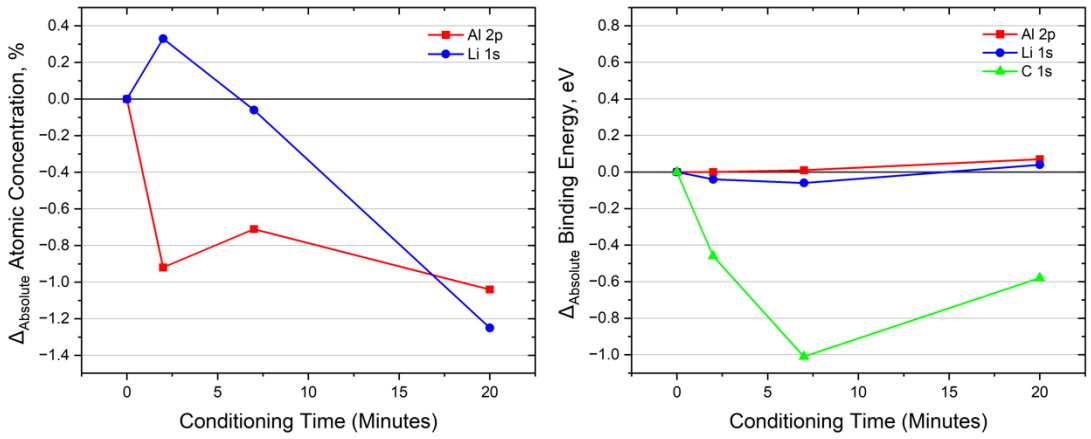

Fig. 8. Absolute changes in atomic concentration (left) and binding energy (right) for select orbitals of spodumene A throughout FA2 conditioning

3.2.2. ToF-SIMS

ToF-SIMS served to characterize changes in surface species on spodumene throughout high-density TOFA conditioning. The normalized intensity measurements of several positive and negatively charged

species on conditioned samples of spodumene A were reported, however, only select species were included in this discussion. Relative changes in the positively charged lithium and aluminum species that are attributed at fatty acid adsorption sites are shown in Fig. 9, while changes in TOFA on the spodumene surface are presented in Fig. 10. The peak positions used to identify TOFA on the spodumene surface were determined through ToF-SIMS analysis of a reference sample of pure TOFA collector in the molecular form. The peaks referenced in this study to discuss relative changes in TOFA concentration on the spodumene surface were 71, 141, 169, and 195 amu.

As the final conditioning pH increased from 6.8 to 7.6, there was a significant increase in lithium and aluminum exposure on the spodumene surface (Fig. 9). A similar increase in silicon exposure was also observed. The exposure was lowest at a final pH of 6.8 and highest at final pH of 7.6 (short and long conditioning time, respectively), indicating the amount of collector on the surface decreased during conditioning. The TOFA results shown in Fig. 10 further support this finding, exhibiting a relative decrease in TOFA on the spodumene surface throughout conditioning. In addition to the peaks at 71, 141, 169, and 195 amu, similar decreases in TOFA adsorption were reported for the remaining peaks identified in the reference TOFA sample (not presented in this manuscript).

Because the reference spectra for FA2 was defined with samples of pure FA2, which contains mainly oleic and linoleic acids in their molecular form, it can be concluded that the molecular forms of the TOFA species were responsible for the trend of decreasing collector adsorption at longer conditioning times reported by ToF-SIMS. Physical adsorption of molecular TOFA was expected within the tested pH range, and according to literature, this physisorption should occur at a greater extent when there is excess molecular fatty acid present compared to the anion (Kulkarni & Somasundaran, 1980; Yap et al., 1981; Moon & Fuerstenau, 2003). The lack of vacuum drying in preparation for ToF-SIMS to preserve the molecular fatty acid and the fatty acid speciation behavior in Fig. 2 strongly supports this argument. According to Fig. 2, the pH range tested in this study (both single mineral and batch flotation) corresponds with the region where molecular TOFA (e.g., insoluble oleic acid) should be the dominating collector species. After two minutes of conditioning (final pH 6.8) the concentration of molecular TOFA should be over 200 times greater than the concentration of the fatty acid anion (oleate anion monomer in Fig. 2), and 200,000 times greater than acid-anion complex). And throughout the 20 minutes conditioning period to pH 7.6, the molecular TOFA concentration should remain at least 20 times greater than the highest concentration of anionic species.

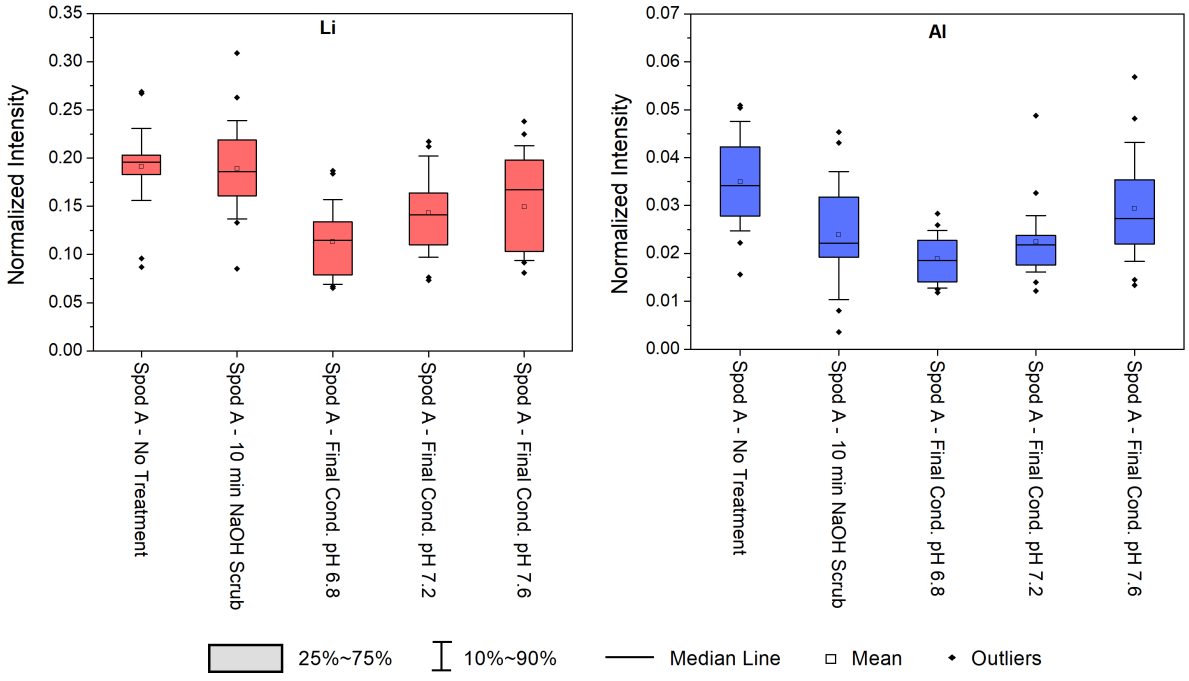

Fig. 9. Normalized ToF-SIMS intensity measurements of lithium (left) and aluminum (right) sites on conditioned samples of spodumene A

The ToF-SIMS results show highest concentration of molecular acid on the spodumene surface occurred at the start of conditioning. Although the arrangement of physically adsorbed collector requires further investigation, several arrangements may occur: a monolayer covering the spodumene surface, a multi-layer on top of chemisorbed fatty acid anion, or a thicker vesicle-type layer made up of several fatty acid molecules (Yap et al., 1981; Fukuda, 2001). However, this coverage is likely varying across the mineral surface. The relative decreases in physically adsorbed collector throughout conditioning (Fig. 10) suggested that this layer was slowly broken up throughout conditioning but remains to some extent after 20 minutes. As this layer was removed or its thickness is reduced, the ToF-SIMS results (Fig. 9) indicated more of the mineral surface was exposed, revealing more lithium and aluminum sites for chemisorption of the anionic species.

While a combination of physicochemical factors was expected to influence the TOFA physically adsorbed on the surface, the dispersion or rearrangement of this phase was most likely governed by the attritioning/emulsifying environment of high-density conditioning and improved solubility at higher pH. In addition to the influence of time and pH behavior (which are reflected in this study), factors like conditioning energy input, impeller and cell design, pulp density, temperature, and collector dosage may impact the TOFA adsorption behavior (Arbiter et al., 1961; Menendez et al., 2004; Cook et al., 2023). Because it was difficult to differentiate between the molecular and anionic fatty acid form, future studies of this system using ToF-SIMS or alternate techniques, should evaluate samples with and without vacuum drying.

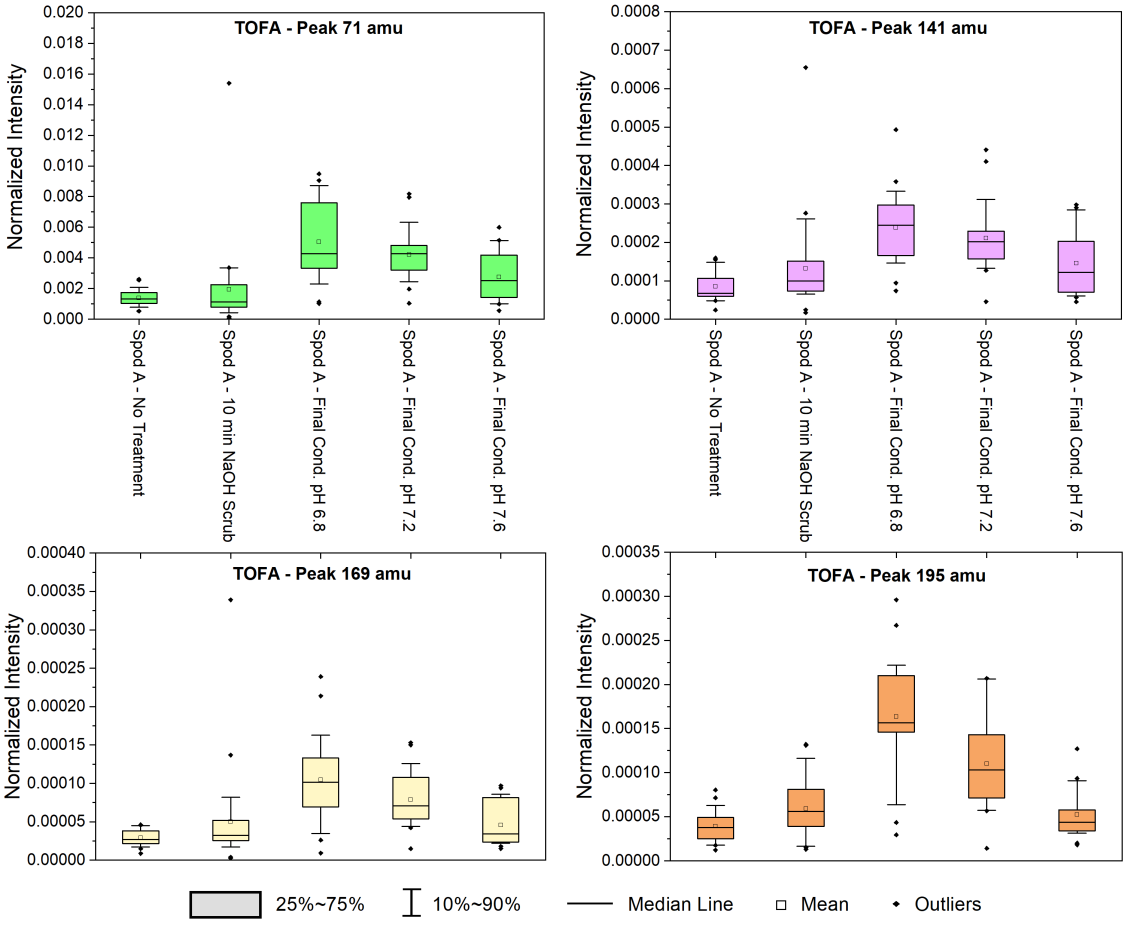

Fig. 10. Normalized ToF-SIMS intensity measurements of TOFA peaks at 71, 141, 169, and 195 amu (clockwise from top right) on conditioned samples of spodumene A

3.3. Batch flotation testing

The six batch flotation tests with real ore (ore A - 1.64% Li_2O and ore B - 1.10% Li_2O) were used to determine how the changes observed using XPS and ToF-SIMS corresponded with laboratory flotation performance. The flotation results for lithium, potassium, and sodium after conditioning to different

final pH values are presented in Fig. 11a., b., and c., respectively, and Table 5 and the relative changes in recovery for each metal are shown in Fig. 11d. The lithium results correspond primarily with spodumene recovery, while the potassium and sodium results are the main indicators of gangue minerals like feldspars. Each ore was conditioned for three different times (3, 7, and 20 minutes), which targeted the final pH values of ~6.7, ~7.1-7.2, and ~7.5-7.7 used in the plots of Fig. 11 to best recreate the final pH values used in single mineral studies. The repetition of each test in triplicate was not possible in this study due to material limitations. However, the standard deviation in flotation performance from the scoping tests with ore A are included in Fig. 11. The four scoping tests reveal strong repeatability in lithium performance with a standard deviation of 0.51 for lithium recovery and 0.04 for Li_2O concentrate grade.

Table 5. Summary of batch flotation results with ore A (1.64% Li_2O) and B (1.10% Li_2O)

Ore Type	Feed Grade (%Li_2O)	Cond. Time (min)	Final pH	Assay (%)				Distribution (%)				
				Li_2O	Fe_2O_3	K_2O	Na_2O	Mass	Li	Fe	K	Na
Ore A – Scoping 1	1.64	10	7.10	4.89	1.02	0.61	1.39	33.4	97.0	81.0	11.9	11.9
Ore A – Scoping 2	1.64	10	7.14	4.93	1.04	0.67	1.35	32.5	96.6	73.6	12.4	11.2
Ore A – Scoping 3	1.64	10	7.12	4.84	1.01	0.70	1.50	33.8	96.7	76.3	13.5	13.0
Ore A – Scoping 4	1.64	10	7.08	4.93	0.94	0.63	1.53	34.6	97.7	62.4	12.7	13.6
Ore A	1.64	3.0	6.68	4.80	0.95	0.66	1.51	34.6	97.2	68.6	13.3	13.4
Ore A	1.64	7.0	7.20	5.07	0.93	0.52	1.25	31.7	96.2	65.2	9.6	10.2
Ore A	1.64	20.0	7.49	5.21	1.00	0.55	1.23	31.0	94.8	64.2	9.9	9.8
Ore B	1.10	3.0	6.72	3.92	2.05	0.88	1.89	26.2	95.7	70.8	18.5	11.4
Ore B	1.10	7.0	7.11	4.28	2.12	0.79	1.69	23.8	94.0	67.5	15.2	9.3
Ore B	1.10	20.0	7.72	4.82	2.38	0.62	1.35	18.0	76.6	57.3	8.9	5.6

The best flotation performance with both ores was achieved after 7 minutes of conditioning to a final pH of 7.1-7.2; both high Li_2O concentrate grades and lithium recoveries were achieved. There was clear evidence that increasing conditioning time and final pH improved rougher concentrate grade (Li_2O) for both spodumene ores, while decreasing the lithium recovery. The concentrate grades for both ores increased at a similar rate with increasing final pH, however, the rate of decreasing lithium recovery differed significantly. For ore A, the overall decrease in lithium recovery between pH 6.8 and 7.5-7.7 was only 2.4% (97.2 to 94.8%), while the decrease for ore B was significantly higher at 29.1% (95.7 to 76.6%). This difference was likely driven by the mineralogy of each ore. The iron data in Table 5 followed a similar trend to lithium with a decrease in recovery and an increase in concentrate grade throughout conditioning, reiterating that selective rejection of iron-bearing minerals is challenging with TOFA collectors.

The potassium and sodium flotation results (Fig. 11b. and c., respectively) followed a similar trend to one another for both ores, decreasing in grade and recovery as conditioning progressed. This differed from lithium where the grade increased, and recovery decreased. The relative percent decrease in potassium and sodium recovery was greater than the relative decrease in mass and lithium recovery throughout conditioning (Fig. 11d.) showing how selective rejection of potassium and sodium improved as conditioning progressed. The greater decrease in mass, potassium, and sodium compared to lithium between 3 and 7 minutes also highlights how silicate gangue rejection was improved in this short interval of conditioning. Overall, the flotation results confirmed that longer conditioning times improved the lithium concentrate grade while decreasing recovery.

3.4. Proposed mechanisms of fatty acid adsorption and dynamic pH behavior

The previous sections highlighted how different minerals exhibit different pH responses during high-density conditioning due to differences in the concentration of cationic surface sites. In addition, the surface studies and batch flotation tests identified other relationships with increasing final conditioning

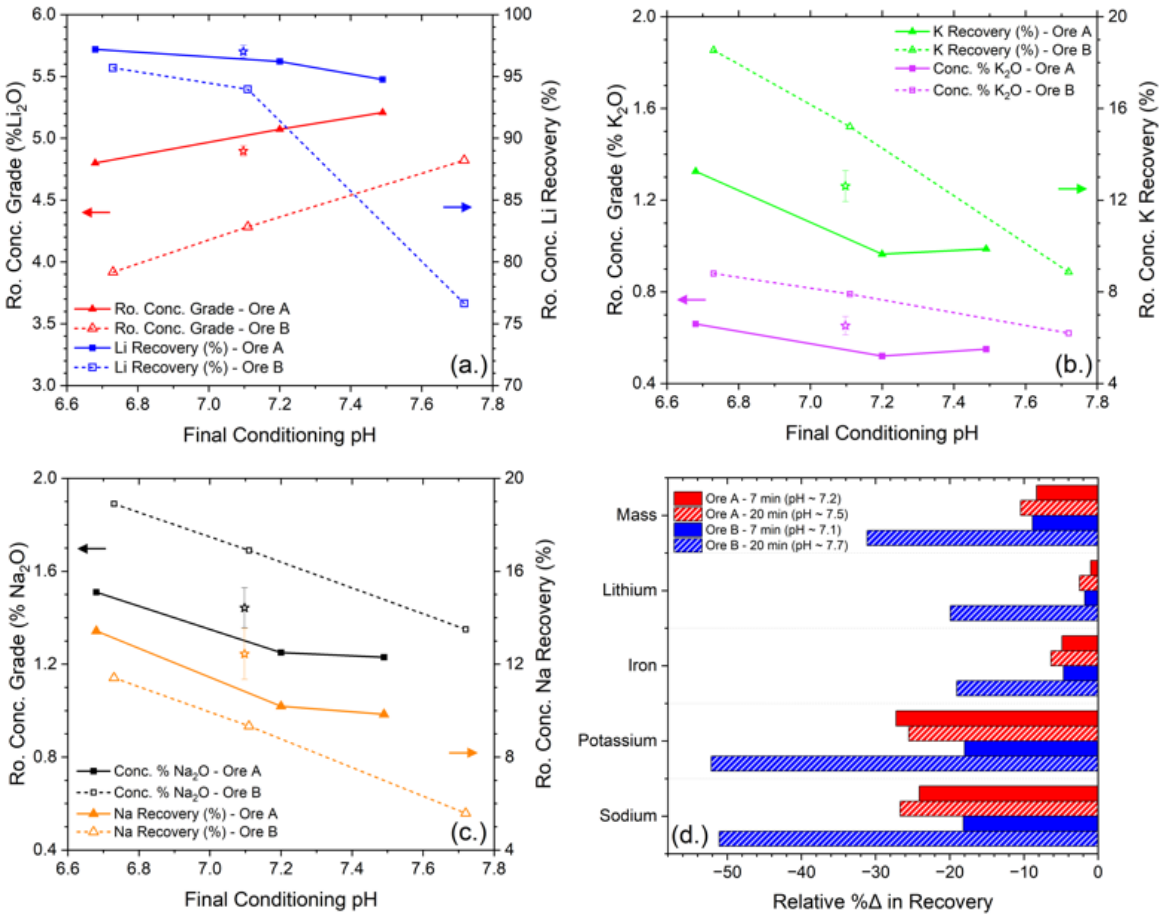

Fig. 11. Rougher concentrate grade and recovery results vs. final conditioning pH for (a.) lithium, (b.) potassium, (c.) sodium, and (d.) the relative change in recovery during conditioning from the performance at final pH 6.8. Star points on plots (a.) through (c.) represent the average performance and standard deviation of the results of the four repeat scoping tests

pH (i.e., conditioning time): (1) a decrease in physisorption of molecular TOFA at the spodumene surface (ToF-SIMS); (2) changing flotation performance where the selectivity significantly increases due to improved gangue rejection but lithium recovery begins to decrease; and (3) potential formation and subsequent dispersion of the fatty acid-anion complex at the spodumene surface (XPS).

The increase in pH over time shown in Fig. 6 is the result of a chemical reaction occurring during conditioning, where the concentration of H+ in solution decreases over time. The greater rate of pH changes during conditioning recorded for minerals with more cationic sites (ex. Al^{3+}, Fe^{3+}, Mg^{2+}, Ca^{2+}, Li+) should correspond with increased TOFA chemisorption as indicated by literature (Yu et al. 2015b; Shu et al., 2020; Meng et al., 2022; Ma et al., 2025; Zhu et al., 2024). However, this TOFA chemisorption does not explain the decrease in H^+, which should occur with the observed increasing pH. A potential explanation for the increasing pH during conditioning can be drawn from the fundamental dissociation equation of oleic and linoleic acids shown in equations 1 to 3.

$$\mathbf{RCOOH_{aq}} \leftrightarrow \mathbf{RCOO^-} + \mathbf{H^+} \quad (1)$$

$$\mathbf{RCOO^-} + \mathbf{RCOO^-} \leftrightarrow \mathbf{(RCOO)^{2-}} \quad (2)$$

$$\mathbf{RCOO^-} + \mathbf{RCOOH} \leftrightarrow \mathbf{RCOO^-} \cdot \mathrm{RCOOH} \quad (3)$$

The immediate drop in pH when TOFA is added to the conditioning cell is caused by dissociation of the molecular acid (RCOOH) in equation 1 since it is the only possible reaction producing H+. According to Le Chatelier's principle, as anionic ($RCOO^-$) chemisorption at mineral surfaces occurs, more anions will be removed from solution with further dissociation of RCOOH into $RCOO^-$ and H^+ to maintain equilibrium, theoretically reducing the pH. Contrarily, in this study, the pH was observed to increase throughout conditioning as molecular acid was dispersed from the particle surfaces and more

sites for collector adsorption were exposed. This directly contradicts Le Chatelier's principle and suggests additional factors are at play.

The electroneutrality principle dictates that ions in solution will balance, meaning any protons will be balanced with negatively charged ions or adsorbed onto a charged surface via surface protonation. Sverjensky et al. (1996) determined that the protonation and deprotonation of silicate surfaces exist in equilibrium but can result in the formation of metal hydroxides like MOH and MOH_2^+. The same surface hydroxyls can be found on spodumene and other silicates like quartz and feldspars which may help to explain the simultaneous increase in pH and chemisorption during conditioning (Sverjensky et al., 1996; Zhu et al., 2020).

The top schematic in Fig. 12 proposes a mechanism for the observed pH increase during conditioning. In the spodumene-water system, water molecules will initially adsorb on the surface and rearrange themselves to balance any uncoordinated cations and form hydroxyl groups (Fukushi et al., 2021). As this happens, any uncoordinated MO^- species gains a proton which reduces its charge to (1) MOH. When fatty acid is introduced into the system, the generation of H^+ in solution may lead to two possible interactions on silicate surfaces in the spodumene system: (1) further protonation of MOH to MOH_2^+ or (2) protonation of remaining exposed O^- on the mineral surfaces.

The first scenario was confirmed by Quezada & Toledo (2021) who used DFT to demonstrate that as H+ is released and adsorbed onto spodumene, $RCOO^-$ will migrate to the mineral surface and exchange

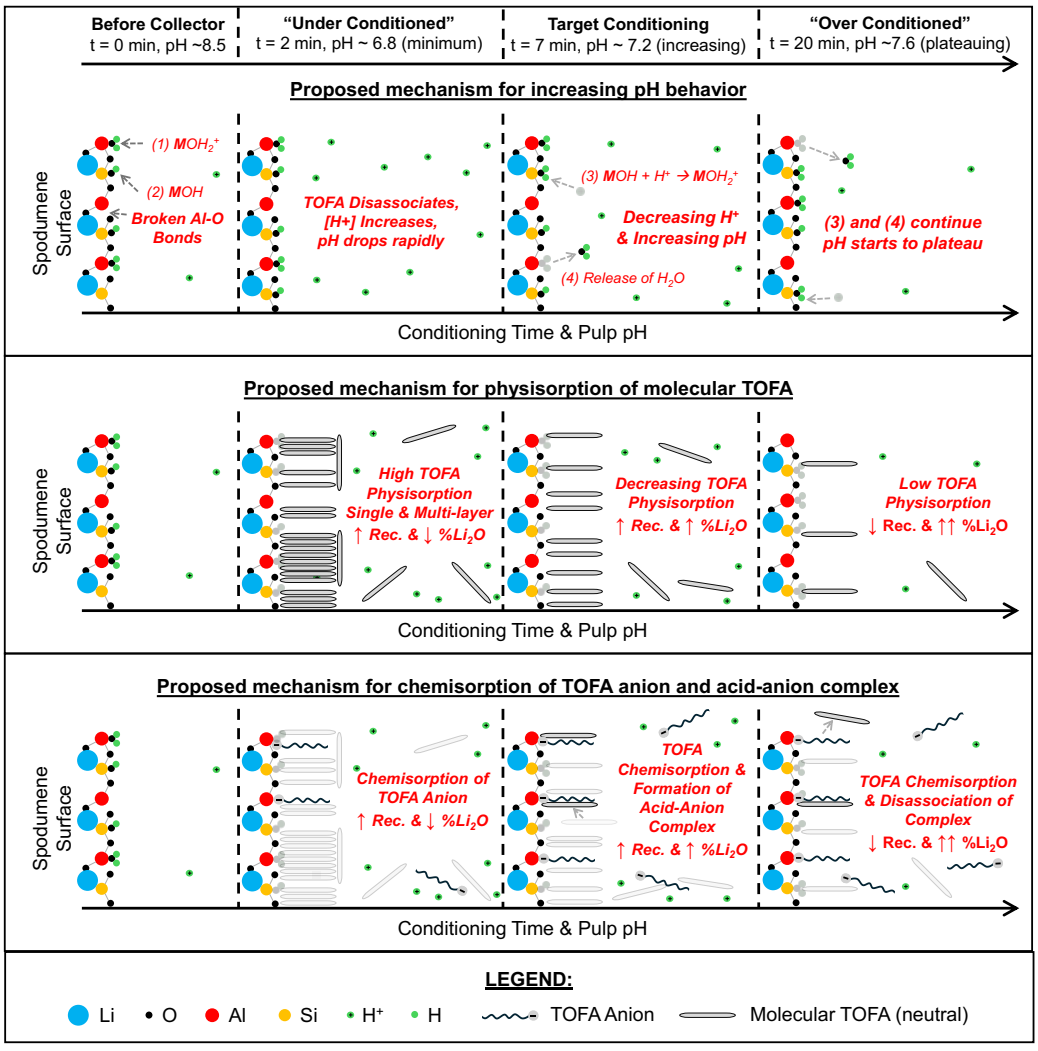

Fig. 12. A schematic of the suggested fatty acid behavior in solution. The proposed mechanism for the increasing pH during high-density conditioning (top) includes: (1) H_2O adsorption onto metal (Al, Si, Li) surface sites forming MOH_2^+; (2) formation of MOH; (3) adsorption of H^+ ions released from fatty acid dissociation to form MOH_2^+; and (4) exchange of H_2O with the fatty acid anion at cationic sites through chemisorption. The proposed physisorption (middle) and chemisorption (bottom) behaviour at the particle surfaces are also included

with H_2O species due to thermodynamic favorability. As this occurs, a neutral water molecule will be released into solution and increase the pH. The production of both $RCOO^-$ and H^+ species in the solution will continue as they are simultaneously adsorbed onto the surface until the available cationic surface sites are consumed. At this point, the pH should plateau, which is best shown by spodumene B in Fig. 6. In the case of quartz, the lack of cationic surface sites for $RCOO^-$ adsorption led to an immediate plateau. But when iron ions were introduced, the pH profile changed dramatically and became comparable to spodumene A and hematite. While it is understood that water molecules should already be covering any exposed O^- on the surface to hinder further protonation, the second scenario may occur after physical adsorption of the molecular acid. The dispersion of the molecular acid off the mineral surfaces could further expose O^- (e.g., on surfaces of spodumene and potentially other silicates) which would further increase the pH without chemisorption.

The XPS and ToF-SIMS data revealed a transformation of the adsorbed fatty acids that occur during conditioning can be directly tied to the batch flotation results. The ToF-SIMS results revealed there was initially high adsorption of molecular acid onto spodumene (Fig. 12, t = 2 minutes), which resulted in a high recovery but a lower concentrate grade. While not evaluated in this study, ToF-SIMS of common silicate gangue minerals in spodumene deposits will be important to evaluate in further studies. From the available results, the lower selectivity after a short conditioning time may be attributed to physical adsorption onto other silicate gangue and potential entrainment due agglomeration of silicate gangue caused by unselective physisorption of the fatty acid. As conditioning progressed, ToF-SIMS demonstrated how the amount of physically adsorbed acid decreased while exposed sites for chemisorption increased, while XPS carbon data suggested that there was an increase in formation of the acid-anion complex. This corresponded with an improved lithium concentrate grade and only a small change in lithium recovery (Fig. 12, t = 7 minutes), achieving the best flotation performance in Fig. 11. This is aligned with the favoured theory in the literature that chemisorption of the acid-anion complex at cationic aluminum sites drives spodumene flotation (Moon & Fuerstenau, 2003; Yu et al., 2015a; Yu et al., 2015b; Zhu et al., 2020; Xie et al., 2021b; Chu et al., 2022). Finally, as the pH approached 7.6, there was further removal of the molecular acid and indications of dissociation of the acid-anion complex, which continued to increase concentrate grade, but began to significantly reduce lithium recovery (Fig. 12, t = 20 minutes). The significant decrease in lithium recovery after 20 minutes conditioning provided clear evidence that the molecular form of fatty acid was needed on the surface at a high level for high spodumene recovery.

Identification of the acid-anion complex as the species responsible for spodumene flotation was originally determined by DFT calculations but is difficult to confirm as its physical measurement on the spodumene surface is challenging. Regardless, it can be speculated that adsorption of the acid-anion complex occurs either by drawing readily available acid-anion complex out of solution, or by the formation of the complex on the spodumene surface at cationic sites during conditioning. At the conditioning pH values investigated in this study (pH 6.7 to 7.7), Fig. 2 shows the $RCOO^-$ concentration (approx. 1.5×10^{-6} to 1.5×10^{-5} M) should be nearly 500 times greater than the concentration of the acid-anion complex (approx. 3×10^{-9} to 3×10^{-8} M) across this pH range, and the concentration of molecular acid should remain around 3×10^{-4} M. Therefore, it might be difficult for the acid-anion complex to outcompete the anion and preferentially adsorb onto the spodumene surface directly from the solution at a concentration high enough to promote flotation. Instead, it appears most likely that flotation is driven by the presence of both species on the surface, which may promote formation of the acid-anion complex but requires a subtle balance of each species to maintain recovery with high selectivity as presented in Fig. 12.

Yu et al. (2015b) demonstrated the acid-anion complexes form due to van der Waals forces between the anionic and molecular fatty acid species, which is something that may occur during high-density conditioning. While further confirmation is needed, if these van der Waals forces are stronger than the physical adsorption of the molecular acid, it could drive the formation of acid-anion complexes on the surface as suggested by the XPS carbon data, especially as the dispersion of molecular fatty acid and chemisorption of the fatty acid anion increase. If complexes form, and are required to float spodumene, the significant decrease in lithium recovery (95.7 to 76.6%) that was observed with ore B as the pH increased to 7.7 suggested that an ideal complex concentration occurred closer to pH 7.1-7.2, and that

the complex can be broken up during high-density conditioning to reduce recovery. This is also supported by changes in the C 1s binding energy throughout conditioning reported by XPS (Fig. 8) where the minimum binding energy of spodumene A occurred after 7 minutes conditioning in FA2 and corresponded with the best flotation performance. After 20 minutes of conditioning (to pH 7.6), the binding energy began to drift towards the blank value and flotation performance decreased, which insinuated the longer conditioning time led to bonding environment changes that negatively impacted spodumene recovery.

The combination of the results from the literature with the batch flotation results and ToF-SIMS and to some extent the XPS studies, provided strong evidence that the interactions between the molecular acid and its anionic form are required for selective spodumene flotation with high recovery. In addition, the ToF-SIMS results revealed there is a clear need for excess molecular fatty acid on the spodumene surface to achieve high recoveries. This may explain low lithium recoveries reported in academic studies using NaOl, as there would little to no molecular form of oleic acid in those systems. This study provides a new perspective on the applications of fatty acid collectors in spodumene flotation and presents valuable insight into the surface activity during high-density conditioning; however, further investigations and molecular simulations are needed to confirm the proposed mechanism.

4. Conclusions

The adsorption behaviour of fatty acid collectors during high-density conditioning of single minerals and real ores was investigated to improve the understanding of mechanisms driving spodumene flotation. The ToF-SIMS, XPS, and batch flotation results determined that the optimum spodumene flotation performance occurs when the anionic and molecular species of fatty acids are both on the spodumene surface at an ideal proportion (final pH 7.1-7.2). At shorter conditioning times and a lower final pH (~6.7), it was speculated that excess molecular acid on silicate mineral surfaces led to poor selectivity and higher recovery of silicate gangue. While longer conditioning times and a higher final pH (~7.5-7.7), the removal of the molecular acid increased selectivity and decreased recovery.

Single mineral conditioning tests revealed a greater increase in pH during conditioning for minerals with more cationic surface sites. Based on Le Chatelier's principle and the electroneutrality principle it was postulated that this pH increase was a product of protonation of silicate surfaces and simultaneous chemisorption of the fatty acid anion onto spodumene surfaces. This was supported by DFT calculations from the literature, however, further investigations using Surface Complexation Models (SCM) such as Triple Layer Models (TLM) or DFT calculations will be required to further validate this theory.

The ToF-SIMS determined the quantity of molecular TOFA on the spodumene surface decreased throughout conditioning, however, XPS provided little evidence of TOFA chemisorption accepted to occur at surface aluminum surface sites. While the presence of the acid-anion complex remained difficult to confirm, the carbon XPS results indicated its concentration on the spodumene surface initially increased during conditioning before disassociating after longer conditioning times – which corresponded with reduced lithium recovery. To supplement the conclusions from this study, future TOFA adsorption work will include total organic carbon (TOC) analysis to quantify the amount of collector on the surface.

The results of this study identified some of the sources for sensitivities observed in spodumene flotation. The importance of molecular fatty acid physisorption on the spodumene surface was highlighted for the first time. It was also determined that conditioning parameters, like pH and time, can be leveraged to achieve the ideal ratio of molecular and anionic species on the spodumene surface (individually or as the acid-anion complex) to achieve selective flotation with high lithium recovery. This study provides valuable insight into how controlled execution of the conditioning stage can help promote favorable collector adsorption and improve flotation performance, supporting the successful operation of the high-density conditioning stage in commercial plants.

Acknowledgements

The authors would like to acknowledge financial support for this project from the Natural Sciences and Engineering Research Council of Canada (NSERC) through an NSERC Discovery Grant RGPIN-2020-04290 and from SGS Canada and Mitacs through the Accelerate Program. We would also like to

acknowledge the Robert M. Buchan Department of Mining at Queen's University for providing infrastructure support.

References

ARBITER, N., ABSHIER, J. R., CRAWFORD, J. W. (1961). *Attritioning and conditioning in spodumene flotation.* Fiftieth Anniversary of Froth Flotation in USA Proceedings, Colorado School of Mines Quarterly, 56, 323-332.

BALE, M. D., MAY, A. V. (1989). *Processing of ores to produce tantalum and lithium.* Minerals Engineering, 2(3), 299-320.

BOUDREAU, S., AUGER, G., TANGUAY, S., CARRIER, A., … LORD, F. (2024). *NI 43-101 feasibility study report for the Moblan lithium project, Eeyou Istchee James Bay Territory, Quebec, Canada.* Sayona Inc., 276-287.

BLANCHET, D., HARDIE, C., LAVERY, M., LEMIEUX, M., NUSSIPAKYNOVA, D., SHANNON, J. M., WOODHOUSE, P. (2012). *Feasibility study update NI 43-101 technical report Quebec Lithium Project.* Canada Lithium Corp., 13-88.

BOWELL, R. J., LAGOS, L., DE LOS HOYOS, C. R., DECLERCQ, J. (2020). *Classification and characteristics of natural lithium resources.* Elements (Quebec), 16(4), 259-264.

BULATOVIC, S. M. (2007). *2-Collectors.* In S. M. Bulatovic (Ed.), Handbook of Flotation Reagents (pp. 5-41). Elsevier.

CAO, M., BU, H., LI, S., MENG, Q., GAO, Y., OU, L. (2021). *Impact of differing water hardness on the spodumene flotation.* Minerals Engineering, 172, 107159.

CHU, H., CHEN, L., LU, D., WANG, Y., ZHENG, X. (2022). *Ultrasonic pretreatment of spodumene with different size fractions and its influence on flotation.* Ultrasonics Sonochemistry, 82, 105889.

COOK, B. K., AGHAMIRIAN, M., GIBSON, C. E. (2023). *Optimization of spodumene flotation with a fatty acid collector.* Minerals Engineering, 204, 108412.

COOK, B. K., AGHAMIRIAN, M., GRAMMATIKOPOULOS, T., GIBSON, C. E. (2024). *The effect of conditioning pH behaviour on spodumene flotation with fatty acids.* Canadian Metallurgical Quarterly.

DELBONI, H. J., LAPORTE, M.-A., QUINN, J., RODRIGUEZ, P. C., O'BRIEN, N. (2023). *Updated NI 43-101 technical report, Grota Do Cirilio lithium project Aracuai and Itinga regions, Minas Gerais, Brazil.* Sigma Lithium Corporation, p. 45.

DUPÉRÉ, M., PEREZ, P., BOYD, A., ANSON, J., GIRARD, P., GAGNON, R. (2018). *NI 43-101 technical report feasibility study on the Whabouchi lithium mine and Shawinigan electrochemical plant.* Nemaska Lithium Inc.

FARLEY, N. (2022). *CasaXPS: Processing software for XPS, AES, SIMS, and more.* CasaSoftware Ltd. http://www.casaxps.com/

FILIPPOV, L., FARROKHPAY, S., LYO, L., FILIPPOVA, I. (2019). *Spodumene flotation mechanism.* Minerals (Basel), 9(6), 372.

FRIEDMAN, H. (2024). *The hornblende mineral group.* https://www.minerals.net/mineral/hornblende.aspx

FUKUDA, H., GOTO, A., YOSHIOKA, H., GOTO, R., MORIGAKI, K., WALDE, P. (2001). *Electron spin resonance study of the pH-induced transformation of micelles to vesicles in an aqueous oleic acid/oleate system.* Langmuir, 17(14), 4223-4231.

FUKUSHI, K., OKUYAMA, A., TAKEDA, N., KOSUGI, S. (2021). *Parameterization of adsorption onto minerals by extended triple layer model.* Applied Geochemistry, 134, 105087.

GAO, J., SUN, W., LYU, F. (2021). *Understanding the activation mechanism of Ca^{2+} ion in sodium oleate flotation of spodumene: A new perspective.* Chemical Engineering Science, 244, 116742.

GIBSON, C. E., AGHAMIRIAN, M., GRAMMATIKOPOULOS, T. (2017). *The removal of iron-bearing silicate minerals from a hard rock lithium ore.* 49th Annual CMP Conference, Ottawa, Ontario.

GOODE, A., BASCOMBE, L., HUTSON, A., TALBOT, B., KNEER, S., KININMONTH, G. (2021). *Galaxy Resources Ltd. – Mt. Cattlin NI 43-101 technical report.* Galaxy Resources Ltd., 231-234.

JASKULA, B. (2024). *Lithium.* U.S. Geological Survey, Mineral Commodity Summaries.

JIA, W., JIAO, F., ZHU, H., XU, L., QIN, W. (2021). *Mitigating the negative effects of feldspar slime on spodumene flotation using mixed anionic/cationic collector.* Minerals Engineering, 168, 106813.

JIE, Z., WEIQING, W., JING, L., YANG, H., QIMING, F., HONG, Z. (2014). *Fe(III) as an activator for the flotation of spodumene, albite, and quartz minerals.* Minerals Engineering, 61, 16-22.

KRATON CORPORATION. (2021). *Sylfat FA2 Tall Oil Fatty Acid. Product data sheet.* Retrieved June 16, 2024 from https://kraton.com/product-sds/shared-files/87806/?SYLFAT-FA2.pdf

KULKARNI, R. D., SOMASUNDARAN, P. (1980). *Flotation chemistry of hematite/oleate system.* Colloids and Surfaces, 1(3), pp. 387-405.

LIU, W., ZHANG, S., WANG, W., ZHANG, J., YAN, W., DENG, J., FENG, Q., HUANG, Y. (2015a). *The effects of Ca(II) and Mg(II) ions on the flotation of spodumene using NaOL.* Minerals Engineering, 79, 40-46.

LIU, W., ZHANG, J., WANG, W., DENG, J., CHEN, B., YAN, W., XIONG, S., HUANG, Y., LIU, J. (2015b). *Flotation behaviours of ilmenite, titanaugite, and forsterite using sodium oleate as the collector.* Minerals Engineering, 72, 1-9.

LIU, Y., LIU, J., PENG, L., CEN, M., LI, F. (2023). *Mechanistic study and application of anionic/cationic combination collector ST-8 for the flotation of spodumene.* Minerals (Basel), 13(9).

MA, Z., XU, L., GUO, W., WANG, D., XUE, K. (2024). *Effects of alkali pretreatment on the flotation of spodumene and feldspar.* Minerals Engineering, 210, 108676.

MENG, J., XU, L., WANG, D., XUE, K., LUO, L., SHI, X. (2022). *The activation mechanism of metal ions on spodumene flotation from the perspective of in situ ATR-FTIR and ToF-SIMS.* Minerals Engineering, 182, 107567.

MCCRACKEN, T., CANOSA, J., BOYKO, K., WILSON, S., DEGAGNE, R. (2021). *NI 43-101 technical report PAK property, Red Lake Mining District, Ontario.* Frontier Lithium Inc., 13-18.

MCCRACKEN, T., CUNNINGHAM, R. (2023). *NI 43-101 technical report mineral resource estimate for the CV5 Pegmatite, Corvette Property.* Patriot Battery Metals Inc., 13.

MENÉNDEZ, M., VIDAL, J., TORAÑO, J., GENT, M. (2004). *Optimisation of spodumene flotation.* European Journal of Mineral Processing & Environmental Protection, 4(2), 130-135.

MOON, K. S., FUERSTENAU, D. W. (2003). *Surface crystal chemistry in selective flotation of spodumene ($LiAl[SiO_3]_2$) from other aluminosilicates.* International Journal of Mineral Processing, 72(1), 11-24.

MUNSON, G. A., ERICKSON, K. L. (1946). *Studies on the flotation of spodumene from the Edison Mine, Keystone, South Dakota (Report of Investigations No. 3892).* U.S. Dept of the Interior, Bureau of Mines.

NATIONAL CENTER FOR BIOTECHNOLOGY INFORMATION. (2024). *PubChem Compound Summary for CID 445639, Oleic Acid.* Retrieved June 16, 2024 from https://pubchem.ncbi.nlm.nih.gov/compound/Oleic-Acid

NATIONAL CENTER FOR BIOTECHNOLOGY INFORMATION. (2024). *PubChem Compound Summary for CID 5280450, Linoleic Acid.* Retrieved June 16, 2024.

NORMAN, J., GIESEKE, E. W. (1940). *Beneficiation of spodumene rock by froth flotation.* American Institute of Mining and Metallurgical Engineers, March 1940.

PELLETIER, C., BOUDREAU, S., BARIL, F., GAUTHIER, P., POIRIER, E., JOYAL, O. (2023). *Rose Lithium-Tantalum Project feasibility study NI 43-101 technical report.* Critical Elements Lithium Corporation.

PUGH, R., STENIUS, P. (1985). *Solution chemistry studies and flotation behaviour of apatite, calcite and fluorite minerals with sodium oleate collector.* International Journal of Mineral Processing, 15(3), 193-218.

QUEZADA, G. R., TOLEDO, P. G. (2021). *Complexation of alkali and alkaline-earth metal cations at spodumene-saltwater interfaces by molecular simulation: Impact on oleate adsorption.* Minerals, 11(1), 12.

REDEKER, I. H. (1981). *Flotation of feldspar, spodumene, quartz and mica from pegmatites in North Carolina, USA (Report No. 8).* 13th CMP Annual Meeting.

SHU, K., XU, L., WU, H., XU, Y., LUO, L., YANG, J., TANG, Z., WANG, Z. (2020). *In situ adsorption of mixed anionic/cationic collectors in a spodumene–feldspar flotation system: Implications for collector design.* Langmuir, 36(28), pp. 8086-8099.

SRK CONSULTING INC. (2023). *SEC technical report summary pre-feasibility study Greenbushes Mine, Western Australia.* Albemarle Corporation.

SVERJENSKY, D. A., SAHAI, N. (1996). *Theoretical prediction of single-site surface-protonation equilibrium constants for oxides and silicates in water.* Geochimica et Cosmochimica Acta, 60(20), 3773-3797.

TADESSE, B., MAKUEI, F., ALBIJANIC, B., LAURENCE DYER. (2018). *The beneficiation of lithium minerals from hard rock ores: A review.* Minerals Engineering, 131, 170-184.

TANHUA, A., SINCHE-GONZALEZ, M., KALAPUDAS, R., TANSKANEN, P., LAMBERG, P. (2020). *Effect of waste rock dilution on spodumene flotation.* Minerals Engineering, 150, 106282.

TIAN, M., GAO, Z., KHOSO, S. A., SUN, W., HU, Y. (2019). *Understanding the activation mechanism of Pb^{2+} ion in benzohydroxamic acid flotation of spodumene: Experimental findings and DFT simulations.* Minerals Engineering, 143, 106006.

WEN, S., MIAO, Y., TANG, Y., SONG, Z., FENG, Q. (2025). *Theoretical and experimental study on high-entropy flotation of micro-fine cassiterite.* International Journal of Mining Science and Technology, 35(1), 19-39.

WINSOME RESOURCES LTD. (2023). *Our assets.* https://winsomeresources.com.au/our-assets/

XIE, R., ZHU, Y., LIU, J., LI, Y. (2021a). *Effects of metal ions on the flotation separation of spodumene from feldspar and quartz.* Minerals Engineering, 168, 106931.

XIE, R., ZHU, Y., LIU, J., LI, Y., WANG, X., SHUMIN, Z. (2021b). *Research status of spodumene flotation: A review.* Mineral Processing and Extractive Metallurgy Review, 42(5), 321-334.

XU, L., HU, Y., TIAN, J., WU, H., YANG, Y., ZENG, X., WANG, Z., WANG, J. (2016a). *Selective flotation separation of spodumene from feldspar using new mixed anionic/cationic collectors.* Minerals Engineering, 89, 84-92.

XU, L., HU, Y., WU, H., TIAN, J., LIU, J., GAO, Z., WANG, L. (2016b). *Surface crystal chemistry of spodumene with different size fractions and implications for flotation.* Separation and Purification Technology, 169, 33-42.

XU, L., PENG, T., TIAN, J., LU, Z., HU, Y., SUN, W. (2017). *Anisotropic surface physicochemical properties of spodumene and albite crystals: Implications for flotation separation.* Applied Surface Science, 426, 1005-1022.

YAP, S. N., MISHRA, R. K., RAGHAVAN, S., FUERSTENAU, D. W. (1981). *The adsorption of oleate from aqueous solution onto hematite.* In Adsorption from Aqueous Solutions. Springer: American Chemical Society, Boston, MA, USA, 119-142.

YU, F.-S., WANG, Y.-H., WANG, J.-M., XIE, Z.-F., ZHANG, L. (2014). *First-principle investigation on mechanism of Ca ion activating flotation of spodumene.* Rare Metals, 33(3), 358-362.

YU, F., WANG, Y., ZHANG, L. (2015a). *Effect of spodumene leaching with sodium hydroxide on its flotation.* Physicochemical Problems of Mineral Processing, 51(2), 745-754.

YU, F., WANG, Y., ZHANG, L., ZHU, G. (2015b). *Role of oleic acid ionic−molecular complexes in the flotation of spodumene.* Minerals Engineering, 71, 7-12.

ZHANG, Y., ZHOU, H., CAO, Y., LUO, X., XIE, F., ZHANG, B., YANG, S. (2021). *Activation mechanism of calcium hydrolysate on the spodumene surface and its effect on the adsorption of collector.* Minerals Engineering, 174, 107221.

ZHAO, J., LUO, H., LIU, Y., LIU, J., PENG, L., CEN, M., LI, F. (2023). *Mechanistic study and application of anionic/cationic combination collector ST-8 for the flotation of spodumene.* Minerals (Basel), 13(9), 1177.

ZHU, G., ZHAO, Y., ZHENG, X., WANG, Y., ZHENG, H., LU, D. (2020). *Surface features and flotation behaviors of spodumene as influenced by acid and alkali treatments.* Applied Surface Science, 507, 145058.

ZHU, G., WANG, R., ZHENG, Y., ZHANG, X., ZHANG, Y., LI, C., LI, G., CAO, Y. (2025). *The adsorption characteristics of calcium ions on Spodumene with Different Colors and Their Associated Activation Mechanism.* Minerals, 15(1), 48.